Aalto University

OPEN ACCESS

This is an electronic reprint of the original article.
This reprint may differ from the original in pagination and typographic detail.

Dubovik, Maria; Warsta, Lassi; Tamm, Ottar; Wendling, Laura; Rinta-Hiiro, Ville; Koivusalo, Harri

Processes influencing stormwater purification by roadside biochar-amended sand filter in cold climate conditions

Published in:
Boreal Environment Research

DOI:
10.60910/t2j9-62jy

Published: 17/01/2024

Document Version
Publisher's PDF, also known as Version of record

Published under the following license:
CC BY

Please cite the original version:
Dubovik, M., Warsta, L., Tamm, O., Wendling, L., Rinta-Hiiro, V., & Koivusalo, H. (2024). Processes influencing stormwater purification by roadside biochar-amended sand filter in cold climate conditions. *Boreal Environment Research*, *29*(1-6), 17-34. https://doi.org/10.60910/t2j9-62jy

This material is protected by copyright and other intellectual property rights, and duplication or sale of all or part of any of the repository collections is not permitted, except that material may be duplicated by you for your research use or educational purposes in electronic or print form. You must obtain permission for any other use. Electronic or print copies may not be offered, whether for sale or otherwise to anyone who is not an authorised user.

BOREAL ENVIRONMENT RESEARCH 29: 17–34
ISSN 1797-2469 (online)
© 2024
Helsinki 17 January 2024

Processes influencing stormwater purification by roadside biochar-amended sand filter in cold climate conditions

Maria Dubovik[1)*], Lassi Warsta[1)], Ottar Tamm[2)3)], Laura Wendling[1)], Ville Rinta-Hiiro[1)] and Harri Koivusalo[2)]

[1)] *VTT Technical Research Centre of Finland, P.O. Box 1000, FI-02044 VTT, Finland*
[2)] *Department of Built Environment, Aalto University School of Engineering, P.O. Box 15200, FI-00076 Aalto, Finland*
[3)] *Institute of Forestry and Rural Engineering, Estonian University of Life Sciences, Kreutzwaldi 5, 51014, Tartu, Estonia*
**corresponding author's e-mail: maria.dubovik@vtt.fi*

Received 14 Jul. 2023, final version received 4 Dec. 2023, accepted 4 Dec. 2023

Dubovik M., Warsta L., Tamm O., Wendling L., Rinta-Hiiro V. & Koivusalo H. 2024: Processes influencing stormwater purification by roadside biochar-amended sand filter in cold climate conditions. *Boreal Env. Res.* 29: 17–34.

Stormwater in Finland typically lacks substantial treatment despite potentially containing elevated concentrations of nutrients and trace metals that can degrade the water quality of receiving waterbodies. Reactive materials, such as biochar, have been effective in removing pollutants from stormwater. However, knowledge of their performance is primarily based upon laboratory tests as field studies remain scarce and there is little evidence on their long-term field performance. This study evaluated field-scale stormwater pollutant retention by sand and biochar-amended sand filtration systems designed to treat road runoff containing metals and nutrients in southern Finland. Results of field data, and hydrological and geochemical modelling suggest that the filters retain pollutants similarly through a combination of physical filtration, (ad)sorption and/or (co)precipitation additionally affected by leaching of alkali metal cations from biochar media which contributed to the formation of new minerals via PO_4^{3-} sorption to Fe (oxy)hydroxides or precipitation of Ca phosphate mineral phases (hydroxyapatite).

Introduction

Urban development is characterised by rapid urbanisation and an expanding footprint of human activities. A substantial body of evidence indicates that urban development has transformed the dynamics of runoff generation in urban catchments both in terms of runoff volume and its composition (e.g., Lundy *et al.*, 2012, Taka *et al.*, 2017). Traffic- and road-originating runoff has been shown to transport a substantial quantity of pollutants from sources including atmospheric deposition, exhaust emissions, tire abrasion and the use of agents such as de-icing salts (Markiewicz *et al.*, 2017, Järlskog *et al.*, 2021). Owing to elevated pollutant concentrations and high variability of urban stormwater composition, nutrients and trace metal contaminants in traffic- and road-originating runoff increase diffuse pollution and environmental degradation of recipient surface waters, and soil- and groundwater resources (Bäckström *et al.*, 2003, Lundy *et al.*, 2012).

Editor in charge of this article: Hannu Marttila

Engineered structures for passive water treatment are widely recognised as a cost-effective means of addressing diffuse pollution. In recent decades, numerous measures to mitigate the adverse impacts of urban runoff on surface waters and groundwater resources have been developed, ranging from structural measures to relatively more integrated approaches such as sustainable urban drainage systems (SUDS) and green infrastructure (see e.g., Fletcher *et al.* (2015) for an in-depth overview). Filtration paired with reactive materials often presents an economical yet reliable solution for enhancing pollutant removal from runoff (Kuoppamäki *et al.*, 2019). Stormwater filtration through chemically reactive geo- and/or bio-based materials, including sand filters amended with biochar, has previously been demonstrated to effectively retain a range of stormwater pollutants (e.g., Reddy *et al.*, 2014, Wendling *et al.*, 2017).

Biochar, a product of biomass pyrolysis or gasification, has been previously employed predominantly for soil improvement and carbon sequestration (Lehmann and Joseph, 2009). Availability of feedstock and low production cost make biochar an attractive environmental sorbent (Ahmad *et al.*, 2014). Biswal *et al.* (2022) highlight that the number of studies evaluating biochar performance from different feedstocks for stormwater treatment has increased over the last decade. Currently, biochar-amended filtration systems are recognised to exhibit superior performance in retaining and immobilising nutrients (Ulrich *et al.*, 2017), metals and metalloids (Ashoori *et al.*, 2019), and even removing pathogenic bacteria (Mohanty *et al.*, 2014). The amendment of biochar is also expected to increase water retention capacity, which can enhance detention of stormwater compared to non-amended filters (Mai and Huang, 2021).

Biochar can be produced at different temperatures, which together with feedstock largely determine its final properties influencing the removal capacity such as pH, ash content, porosity and cation exchange capacity (Kaya *et al.*, 2022). Studies have shown that stormwater pollutant removal capacity improved with increasing biochar production temperature (Spahr *et al.*, 2022). Biochar characteristics such as surface area, hydrophobicity, number of functional groups, and to a certain extent ash content, influenced by pyrolysis/gasification temperature, affect the adsorption of pollutants (Kaya *et al.*, 2022; Spahr *et al.*, 2022).

Previous investigations of biochar-amended stormwater filtration systems predominantly involved column-type laboratory, batch-scale or pilot testing of material performance using synthetic stormwater (e.g., Genç-Fuhrman *et al.*, 2007, Ashoori *et al.*, 2019, Siipola *et al.*, 2020). For example, Ashoori *et al.* (2019) and Tian *et al.* (2016) demonstrated substantial (> 90%) ammonia nitrogen (NH_4-N) and nitrate nitrogen (NO_3-N) removal in column-based tests. Removal of phosphorus (P), however, is variable and it depends on the biochar feedstock (Afrooz and Boehm, 2017), pore volume for facilitating adsorption, and the presence of an additional metal coating, which has been demonstrated to enhance P adsorption (Xiong *et al.*, 2019). The biochar production temperature and the nutrient content of its feedstock additionally influence the biochar filtration system performance in removing stormwater pollutants and its longevity (Boehm *et al.*, 2020). Biochar media has also been investigated as the green roof substrate to reduce nutrient loading in both roof runoff and green roof leachate (Kuoppamäki and Lehvävirta, 2016, Liao *et al.*, 2022).

Biochar has additionally been studied for removal of metals from stormwater. Biochar with varying feedstock have demonstrated the ability to retain heavy metals such as cadmium (Cd), lead (Pb), copper (Cu) and zinc (Zn) and their adsorption increased with biochar application rate (Komkiene and Baltrenaite, 2016, Ashoori *et al.*, 2019). Similarly, Kołodyńska *et al.* (2012) observed the adsorption of the same metals, and pH influence on the adsorption of metals. They concluded that higher pH reduces the adsorption capacity due to precipitation or formation of hydroxide complexes (Kołodyńska *et al.*, 2012). As most metals and P species in street and/or road stormwater runoff exist in particle-bound form (Owens and Walling, 2002), both physical entrapment and biogeochemical reactions influence pollutant dynamics within urban stormwater filtration systems. Understanding of ion interactions with mineral and

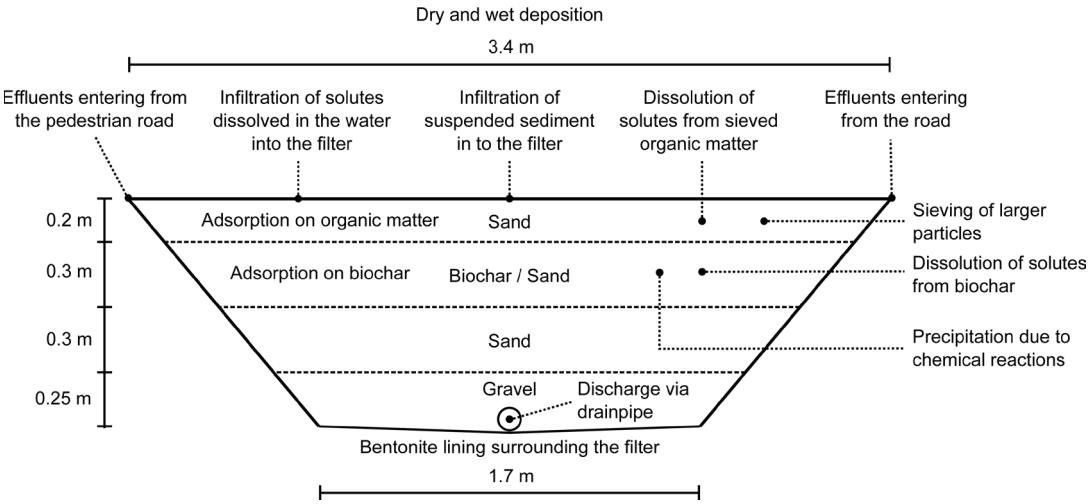

Fig. 1. Cross-section of the sand and sand-biochar stormwater filtration systems and conceptual inputs and outputs of the system.

organic phases is necessary to identify their role in attenuation of targeted pollutants (Wendling and Holt, 2020). Despite the significant experimental research concerning the suitability of filtration media for stormwater pollution retention, there is a notable scarcity of field observations (Biswal *et al.*, 2022). To date, relatively little knowledge exists on the long-term (spanning more than a year) biochar filter performance in field conditions dominated by varying pH and redox conditions (Mohanty *et al.*, 2018).

The objective of the present study was to assess the effects of two adjacent roadside filters on stormwater quantity and quality and understand the pollutant retention and removal processes and subsequently suitable maintenance programme during a continuous period over northern, cold-climate autumn-winter. Both filters had a similar overall structure with the only difference that the sand-biochar filter contained a 300 mm layer of biochar, facilitating comparison of effluent water quantity and quality between filters. The effects of both filters on water quality and pollutant removal were assessed by geochemical modelling. Distributed hydrological modelling was used to verify measured discharge quantities from the filters, and to evaluate whether filters were under saturated conditions for a prolonged period, which would promote anoxic conditions and dissolution of adsorbed pollutants into the discharged waters.

Material and methods

Study site and data

The study site is located in the city of Vantaa, southern Finland (60.31436 N, 24.88096 E). Adjacent areas draining and directly contributing runoff to the filter system include a section of Tikkurilantie, a moderately busy road with an average annual daily traffic load of ca. 7000 vehicles, and a bicycle path (Assmuth *et al.*, 2019). Two identical roadside filters (3.4 m × 10 m each) installed in parallel were constructed in 2017 with differing filter media: sand and sand-biochar media (powdered biochar from birch wood, *Betula* spp.) (for details see Assmuth *et al.*, 2019, Fig. 1). The particle size distribution of sand was 0.2–2 mm, the powdered birch biochar was < 2 mm, and subsurface drain gravel was 8–16 mm. Filters were located next to one another and separated by a bentonite layer to prevent water transfer between the filters. Filters were additionally lined with bentonite to prevent infiltration to and from the surrounding soil, allowing water to flow directly to the subsurface drains located at the bottom of each filter. No core samples were taken from the filters to ensure the integrity of the layering. Thus, it was assumed the layering of the filter media has not significantly changed with time or been substantially affected by external factors, such as compression by foot or vehicle traffic.

The inflow stormwater quality was measured from a bridge via an opening in the bridge drainage structure at ca. 300 m distance from the filters. Precipitation was recorded *in-situ* with two high-resolution rain gauges (IM523 Metos, Pessl Instruments, Austria) at five-minute intervals. Discharge was measured with tipping bucket gauges (TB/0.5L, HyQuest Solutions, Australia) recording flow at five-minute intervals. Pulse counter recorded tips of a tipping bucket gauge with one tip equal to 0.5 L. Inflow to a filter from the street was calculated to originate from an estimated catchment area of 74.5 m^2 which was optimised with PEST (Model-Independent Parameter Estimation and Uncertainty Analysis ver. 13, Doherty, 2010), which facilitates calibration in numerical modelling. The precipitation and discharge were measured with high temporal resolution from autumn 2019 (19 Sep.) to winter 2020 (19 Feb.). The studied period included three measurement campaigns in autumn 2019 for sampling stormwater influents and filter effluents during rainfall events. The campaigns were launched based on weather forecasts to catch stormwater quality during rainfall-runoff events (Table 1). Some precipitation measurements are missing for Event 1 due to equipment malfunction.

During the measurement campaigns, water samples were collected manually using 1 L containers during the three rain events. In total, 10 samples each of sand and sand-biochar filter effluents were collected along with five stormwater samples per a single rain event. In October 2019, each event produced 25 water samples within 15–20 minutes intervals or less, totalling 75 water samples over three rain events (Table 1).

The filters' performance was analysed using the individual results of all ten samples of each filter effluent (instead of other means, e.g., analysing the event mean concentrations) for greater understanding of variability in stormwater quality and filters response in terms of water quality and quantity. Mass balance and the charge balance error percentage (%CBE) were evaluated to determine the accuracy of each sample. Stormwater quality analyses were performed by MetropoliLab Oy and in Aalto University water laboratory in October 2019. Details on water

Table 1. Sampling details and ambient conditions during the sampling events. "Sand-biochar" denotes sand-biochar filter effluent, "Sand" denotes sand filter effluent, and "Stormwater" denotes stormwater influx collected at bridge opening.

Event	Water Sample	Time of sampling (start–end)	No. of samples	Antecedent dry days	Cumulative rainfall/ max rain intensity
1	Sand-biochar	01.10.2019 (04:27)–01.10.2019 (06:42)	10	12 h	10 mm / 0.9 mm h^{-1}
	Sand	01.10.2019 (04:26)–01.10.2019 (06:50)	10		
	Stormwater	01.10.2019 (04:24)–01.10.2019 (05:30)	5		
2	Sand-biochar	20.10.2019 (20:15)–21.10.2019 (07:53)	10	1–2 days	11 mm / 0.6 mm h^{-1}
	Sand	20.10.2019 (21:55)–21.10.2019 (07:58)	10		
	Stormwater	20.10.2019 (19:15)–20.10.2019 (20:15)	5		
3	Sand-biochar	26.10.2019 (15:25)–26.10.2019 (17:05)	10	1–2 days	11 mm / 0.5 mm h^{-1}
	Sand	26.10.2019 (15:45)–26.10.2019 (17:21)	10		
	Stormwater	26.10.2019 (15:05)–26.10.2019 (15:45)	5		

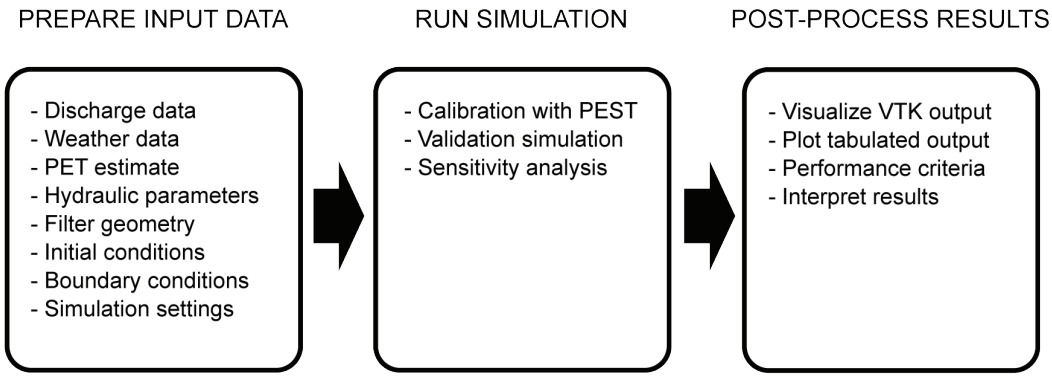

Fig. 2. Flow chart of the STYX model application. Abbreviations: PET = evapotranspiration, PEST = Model-Independent Parameter Estimation and Uncertainty Analysis and VTK = visualisation toolkit.

quality analysis can be found in Koivusalo *et al.* (2023). The water quality data of the stormwater filter outflow and the inflow (bridge drainage water) are summarised in Supplementary Information Fig S1.

Modelling discharge and mineral formation in the filters

To verify the measured discharge and to check the saturation of the filter media, a numerical soil-hydrological model (STYX; Fig. 2) was developed with C++ to simulate relevant processes in Nordic conditions outside and within the filter structure (see Fig. 1). The model has been published as open source (MIT license) software on GitHub. The simulated system was divided accordingly into surface and subsurface domains similar to the FLUSH model (Warsta *et al.*, 2013). STYX describes storage of water in the surface domain, and unsaturated and saturated water flow, and heat conduction in the subsurface domain. Parameter optimisation and sensitivity analysis were performed with the PEST software suite (ver. 13, Doherty, 2010). The input and output computational grids were presented in the Visualization Toolkit (VTK) format (http://www.vtk.org). Goodness of fit of model calibration and validation outputs against the measured discharge were determined with Nash-Sutcliffe efficiency (N-S) coefficient (Nash and Sutcliffe, 1970).

The governing partial differential equations in STYX were numerically solved with the finite volume-based method. In this application, a single rectangular cell was used to store water on the filter surface domain. The tridiagonal algorithm was used to directly solve the resulting equations in the subsurface domain in a 1D column of hexahedral cells (e.g., Warsta *et al.*, 2013). Brute force iterative solvers were also included for comparison purposes. Unsaturated water flow in the subsurface domain was simulated with the Richards equation (Richards, 1931) and saturated water flow with the Darcy equation. Unsaturated hydraulic conductivity and water retention capacity of the soils, i.e., the non-linear relationship between pressure head and water content, were computed using the van Genuchten methods (van Genuchten, 1980). Heat transport was simulated with a modified conduction-convection equation (Warsta *et al.*, 2012). Potential daily evapotranspiration was pre-computed using the Hargreaves equation (e.g., Hargreaves and Allen, 2003).

Water flow in the filters is presented in the model in the following way. Precipitation is scaled with a factor to address the larger catchment area of the filter than the filter top surface. Water accumulates on the surface domain cell. Water in the surface domain infiltrates into the top subsurface cell in the subsurface domain. To promote infiltration from the surface to the subsurface domain, hydraulic conductivity of the top subsurface cell is always considered to be in a saturated state. Evaporation from the subsur-

face domain is removed from the top cell of the subsurface domain. In moist conditions, water percolates through the unsaturated soil towards the bottom of the filter. In dry conditions, water can move upwards in the filter towards the top cell in the subsurface domain where water is removed by evaporation. Water is removed from the filter via a subsurface drainpipe when the cell where the pipe is located becomes saturated.

The dominant pollutant removal mechanisms based on the discharge from both filters were evaluated with mineral saturation indices that indicate possible mineral precipitation or dissolution in PHREEQC software (Appelo and Postma, 2007). Thermodynamic equilibria combined with knowledge of mineral formation kinetics, filter material composition and birch biochar surface reactivity informed the evaluation of pollutant retention mechanisms within the biochar filter matrix. Since the water samples were taken in October, the water temperature was assumed to be 5°C. Discharge from both filters was taken as the input in PHREEQC for the assessment of saturation indices to understand what minerals likely control the effluent concentrations with respect to ambient conditions.

Saturation indices indicate either oversaturation (SI > 0; mineral precipitation) or undersaturation (SI < 0; mineral dissolution) of the mineral phases, whilst SI values between –0.5 and 0.5 represent mineral phase equilibrium with the solution. Saturation indices are calculated as:

$$\mathrm{SI} = \log\left(\frac{\mathrm{IAP}}{K_\mathrm{S}}\right), \quad (1)$$

where IAP is the ion activity product (describes the non-equilibrium state of a solution, i.e., measured concentrations) and K_S is the solubility product (describes the relationship of the ion equilibrium in the solution). SI represents the ratio between the deviations from the evaluated conditions (IAP) to the equilibrium situation (K_S) (Appelo and Postma, 2007).

Results

Hydrological processes

For STYX calibration, the measured drain discharge data was divided in half into calibration (19 Sep.–30 Nov. 2019) and validation data sets (1 Dec. 2019–19 Feb. 2020). Hydraulic conductivity of the sand, catchment area and potential evapotranspiration (PET) multiplier were calibrated automatically with PEST using the sand filter discharge data. Water retention curves (WRC) were manually tested and selected between PEST runs due to the complicated interconnectivity between WRC parameters (Table 2). The sand WRC was selected with trial-and-error basis. Several biochar amended soil WRCs were tested for the biochar layer, but none performed as well as the sand WRC and, in the end, it was retained (Table 2). Hydraulic conductivity of the biochar layer in the biochar filter model was also calibrated with PEST while sand parametrisation, evaporation multiplier and catchment area were derived directly from the sand filter calibration. The successful interoperation of these parameters including catchment area (74.5 m^2) in both filters increased confidence in the calibrated values. The PET value was not scaled down by PEST and the small wintertime PET value was extracted as such from the top cell. The effect of grid resolution was then tested by running the simulations with two different grid resolutions (21 vertical cells with 0.05 m cell depth and

Table 2. Water retention curves applied in the sand and biochar filter layers (see Fig. 1). θ_S and θ_R are the saturated and unsaturated water contents, respectively, α and *n* are van Genuchten water retention curve parameters, and K_S is the saturated hydraulic conductivity.

	θ_S ($m^3\ m^{-3}$)	θ_R ($m^3\ m^{-3}$)	α (m^{-1})	*n* (–)	K_S ($m\ s^{-1}$)
Biochar	0.31	0.02	13.58	1.83	0.0014
Gravel	0.30	0.01	7.00	2.00	0.0056
Sand	0.31	0.02	13.58	1.83	0.0056

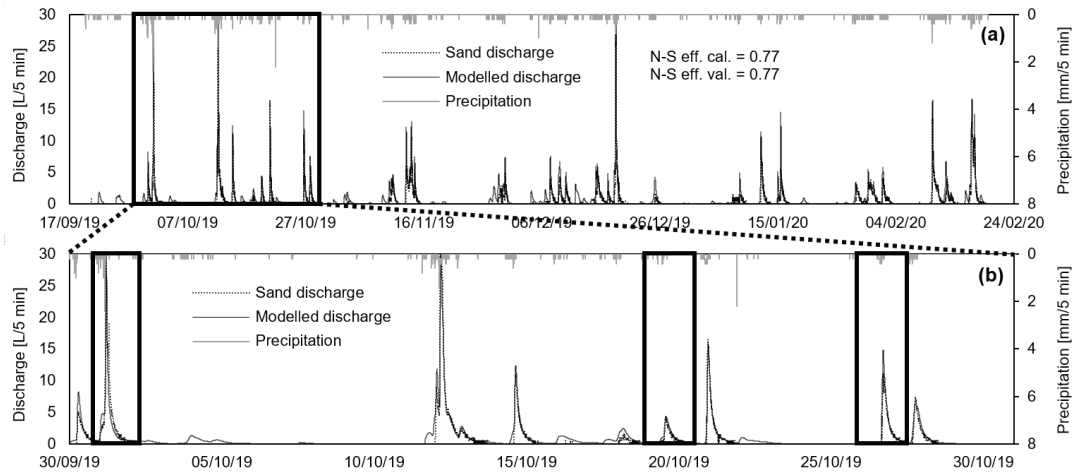

Fig. 3. Cumulative 5-min subsurface drain discharge from sand filter (simulated and measured) and precipitation (corrected series 1) for (**a**) October 2019 and (**b**) discharge over a five-month interval. Measured events are highlighted in thick black squares. N-S eff. cal./val. denote Nash-Sutcliffe efficiencies for calibration/validation, respectively.

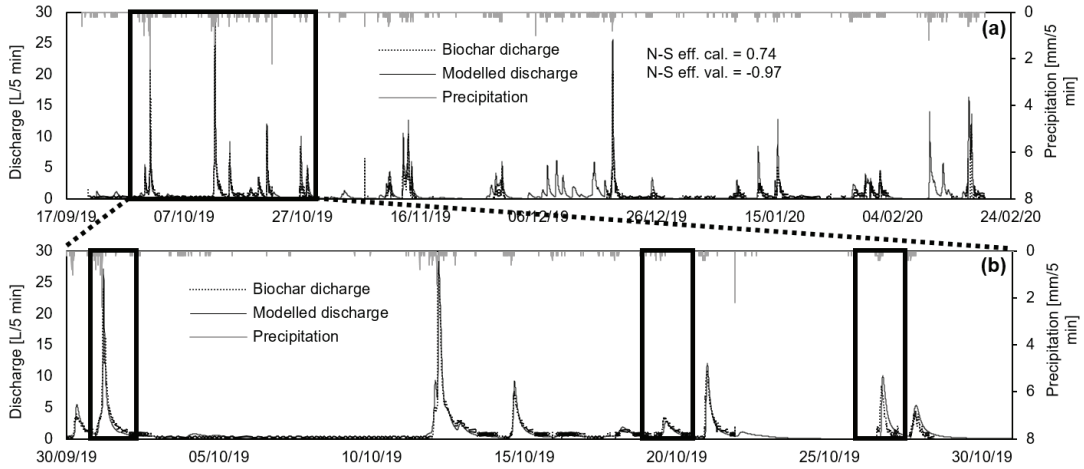

Fig. 4. Cumulative 5-min subsurface drain discharge from sand-biochar filter (simulated and measured) and precipitation (corrected series 1) for (**a**) October 2019 and (**b**) discharge over a five-month interval. Measured events are highlighted in thick black squares. N-S eff. cal./val. denote Nash-Sutcliffe efficiencies for calibration/validation, respectively.

42 cells with 0.025 m cell depth), and according to the results the differences were relatively small.

According to the computed Nash-Sutcliffe model efficiency coefficient (N-S) values (Nash and Sutcliffe, 1970), the sand and biochar models were calibrated successfully against the measured discharge data (Figs. 3 and 4). The validation N-S value for the sand-biochar filter was below zero because several events were missing from the data due to unknown reasons (possibly device malfunction because the peaks were present in the sand filter). The modelled water balance over 19 Sep. 2019 to 19 Feb. 2020 for both filters was similar (sand/sand-biochar, if not stated otherwise): 35.4 m^3 inflow, 1.51 m^3 evaporation, 33.89 m^3/33.86 m^3 discharge, 0.14 m^3/0.18 m^3 storage change, 0.14 m^3/0.15 m^3 error, implying the ability of biochar material to hold more water. Increasing the upper boundary of gravel saturated hydraulic conductivity in the optimi-

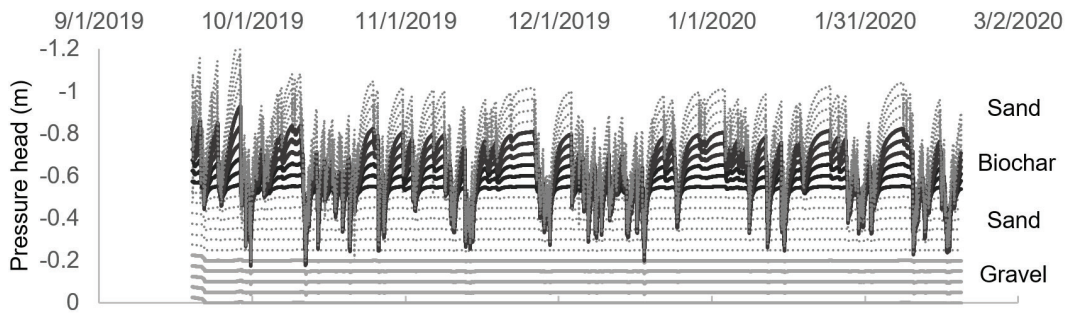

Fig. 5. Pressure head (h) (m) in the filter profile as a function of time. h in the Drainpipe at the bottom of the gravel layer is 0 m (air pressure) and h decreases (suction increases) linearly with elevation in equilibrium conditions. In the results, the profile is always unsaturated ($h < 0$ m) but precipitation events increase h in the upper layers creating non-equilibrium conditions and a hydraulic gradient in the profile inducing flow.

sation stage (Table 2) did not improve the fit of the modelled discharge, and the hydraulic conductivity of gravel and sand remained the same.

The high hydraulic conductivity of the gravel layer and the installed drainpipe at the bottom of the filters ensured that the gravel layer stayed in unsaturated state during the whole simulation period (Fig. 5). The unsaturated gravel layer also enabled the overlaid sand layer in both filter types to drain vertically without restrictions during all assessed precipitation events. This prevented the formation of prolonged saturated conditions in the upper parts of the filter. The biochar filter profile does not get saturated at any point during the simulation (Fig. 5), which can be attributed to gravel intersecting the advancing of the saturation front.

Pollutant removal and retention in view of water quality data

Both the sand-biochar and sand filter effluents consistently exhibited elevated pH and electrical conductivity (EC) relative to the bridge (i.e., reference) stormwater influent (Fig. 6). Over the three studied events, the sand-biochar filter effluent had pH in a range of 7.89–8.16 with average of 8.0, and sand filter effluent in a range of 6.77–7.8 with average of 7.61. Reference raw stormwater had an average pH of 6.74 over three events. Sand-biochar filter exhibited more alkaline conditions in the effluent and significantly higher EC than the sand filter effluent, which had more neutral conditions.

An imbalance between anions and cations was observed in both filter effluents, indicating an additional source of anions not accounted for in measured analytes. Effluent data from the sand and sand-biochar filters demonstrated significant differences with respect to potassium (K^+), total organic carbon (TOC), magnesium (Mg^{2+}), and calcium (Ca^{2+}) concentrations (see Supplementary Information Fig. S1 and Koivusalo *et al.*, 2023) with biochar amended filter leaching a median of 26 mg/L Ca and 11 mg/L K in 2019 data. These differences in effluent concentrations of alkali and alkaline earth metal ions (Ca^{2+} and K^+) illustrate differences in the reactivity of ions within the filter material solid phase capable of buffering acidity. The sand-biochar filter effluents exhibited a greater excess charge of 3.2 mmol/L than the sand filter effluent (ca. 2 mmol/L).

Despite the filters' ability to retain and attenuate metals, such as lead, and nutrients, Koivusalo *et al.* (2023), who studied the same filter structures, observed that the sand and sand-biochar filter effluents demonstrated significant differences with respect to K, TOC, chlorine (Cl), Mg, and Ca, with biochar contributing to elevated concentrations of these elements in the sand-biochar filter effluent relative to the sand filter. Koivusalo *et al.* (2023) reported elevated concentrations of NO_3-N, total nitrogen (TN) and chloride (Cl^-) for the sand filter during high intensity rain events compared with reference stormwater and effluents from the sand-biochar filter. They also observed that biochar amended sand filter demonstrated higher NH_4-N and TN removal.

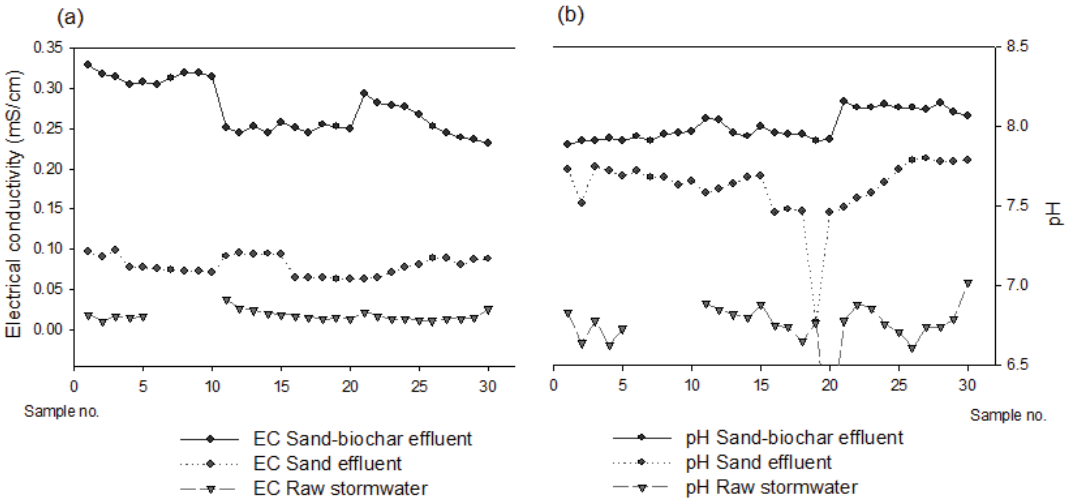

Fig. 6. Electrical conductivity (**a**) and pH (**b**) of raw stormwater, and sand and sand-biochar filter effluents in 2019.

The water quality data (see Supplementary Information Fig. S1) suggested that the filters successfully retained total suspended solids by physical entrapment. This process most likely occurred in the uppermost sections of the filters as sand layers of both filters are comprised of regular grain size (0.2–2 mm), so only particles that can pass downwards can engage in cation exchange with the reactive biochar layer. This implies that sediments and organic matter originating from the walkway and road are accumulating in the upper layers of the filters. Adsorption of metals likely occurs in the top sand layer of the filter containing organic matter at a depth of 0.2 m, and in the biochar layer in the sand-biochar filter (depth of 0.2–0.5 m; Fig. 1). The results further indicate that some of the solutes are dissolving from the filter materials and reacting with the infiltrating solutes, for example total phosphorus (TP) and alkali and earth metals (Ca^{2+} and K^{+}).

Pollutant removal and retention mechanisms based on modelling

The saturation of mineral phases within the sand and sand-biochar filters was simulated for three rain events in October 2019. The interpretation of the modelled data provides information about sorption/desorption and precipitation/dissolution processes occurring inside both filters, which is relevant to understanding the contaminant attenuation capacity and long-term filter performance.

PHREEQC analyses showed that, within filter materials, the degree of iron oxide mineral phase saturation and the quantity of available calcium had a substantial impact on P removal from stormwater via calcium phosphate mineral formation and/or adsorption to iron oxide mineral surfaces in both filters. Influent stormwater and effluents from the filters contained redox-active elements such as manganese (Mn), iron (Fe) and sulphur (S). Their significance lies in the ability of associated Mn, Fe and S mineral phases to engage in a variety of electron-transfer reactions as well as the potential for mineral phase transformations due to changes in redox conditions (Fig. 7). The relative significance of redox-active mineral phases provides knowledge about the environmental conditions necessary to maintain optimum filter performance and informs required maintenance actions.

The mineral phases determined by PHREEQC modelling as most likely controlling major ion concentrations in sand-biochar effluent via precipitation/dissolution reactions included amorphous $Al(OH)_3$, poorly crystalline $Fe(OH)_3$, hydroxyapatite ($Ca_5(PO_4)_3OH$), calcite ($CaCO_3$), MgAl hydrotalcite ($Mg_6Al_2(OH)_{16}(OH)_2$) and MgFe hydrotalcite ($Mg_6Fe_2(OH)_{16}(OH)_2$) (Fig. 8).

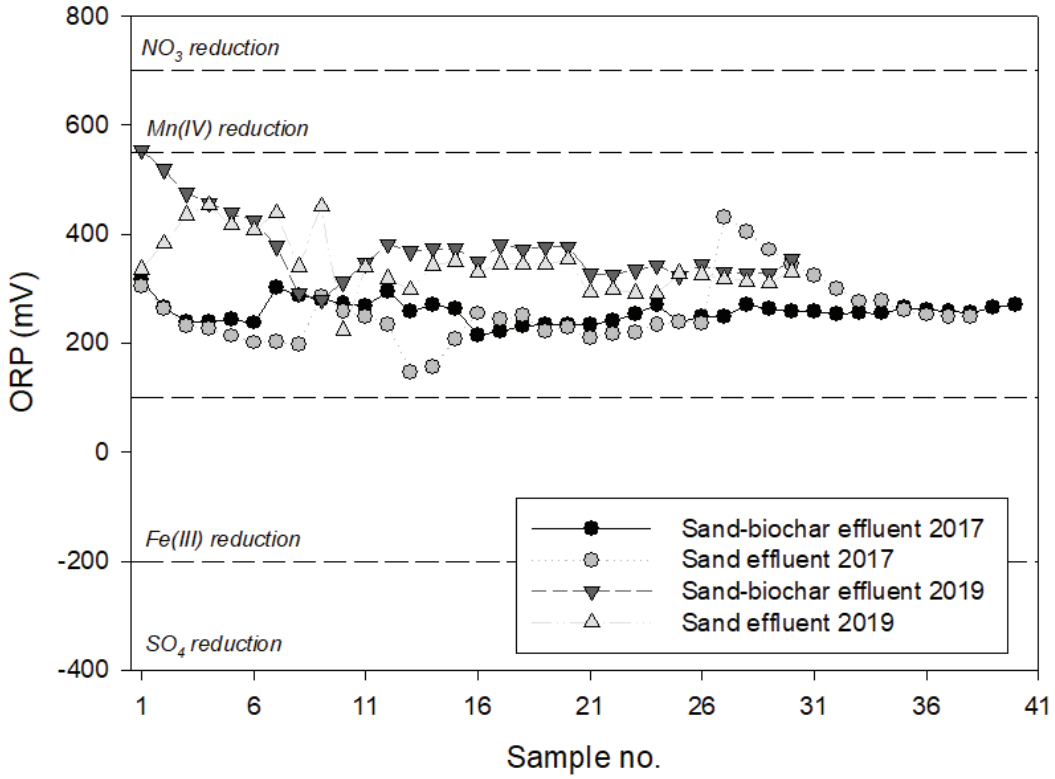

Fig. 7. Measured oxidative-reductive potential (ORP) of sand and sand-biochar filters effluents for all rain events in 2017 and 2019 with approximate zones of nitrate, Mn+4, Fe+3 and sulphate reduction.

The sand and sand-biochar filters exhibited similar aluminium (Al) mineral phase dynamics, with $Al(OH)_3$ most likely controlling Al concentrations. At alkaline pH, alunite ($KAl_3(SO_4)_2(OH)_6$) and gibbsite ($Al(OH)_3$) were the most theoretically stable minerals; however, amorphous $Al(OH)_3$ was most likely the mineral phase controlling Al concentrations due to its lesser degree of crystallinity and more rapid formation in comparison with gibbsite or alunite. Amorphous $Fe(OH)_3$ also has a poorly-crystalline structure that favours its formation in the short term over more crystalline phases. Ferrous iron (Fe^{2+}) forms hematite (ferric iron oxide, Fe_2O_3) and other Fe oxide and oxyhydroxide minerals (e.g., goethite, FeOOH) may also form when oxidized or hydrolysed (Cornell and Schwertmann, 2003), both of which were supersaturated (results not shown). Both the sand-biochar and sand filters exhibited similar oversaturation of ferrihydrite (amorphous $Fe(OH)_3$), goethite (FeOOH), hematite (Fe_2O_3) and schwertmannite ($Fe_8O_8(OH)_6SO_4$).

Sand-biochar effluent showed oversaturation to a near-equilibrium of hydroxyapatite ($Ca_5(PO_4)_3OH$) for all three events and equilibrium or near-equilibrium of calcite ($CaCO_3$) minerals (Fig. 8). Hydroxyapatite and calcite were likely the mineral phases controlling Ca concentrations in the sand-biochar filter effluent, which exhibited 30 times greater effluent Ca concentrations than the sand filter effluent. The saturation of Mg mineral phases indicates a similar dynamic for sand-biochar and sand filter. For all events, MgAl hydrotalcite ($Mg_6Al_2(OH)_{16}(OH)_2$) and MgFe hydrotalcite ($Mg_6Fe_2(OH)_{16}(OH)_2$) remained oversaturated and were likely to have formed *in-situ* during the period of filter operation, whereas other Mg mineral phases such as brucite ($Mg(OH)_2$), talc ($Mg_3Si_4O_{10}(OH)_2$), chrysotile ($Mg_3(Si_2O_5)OH_4$) and sepiolite ($Mg_4Si_6O_{15}(OH)_2 \cdot 6H_2O$) remained undersaturated.

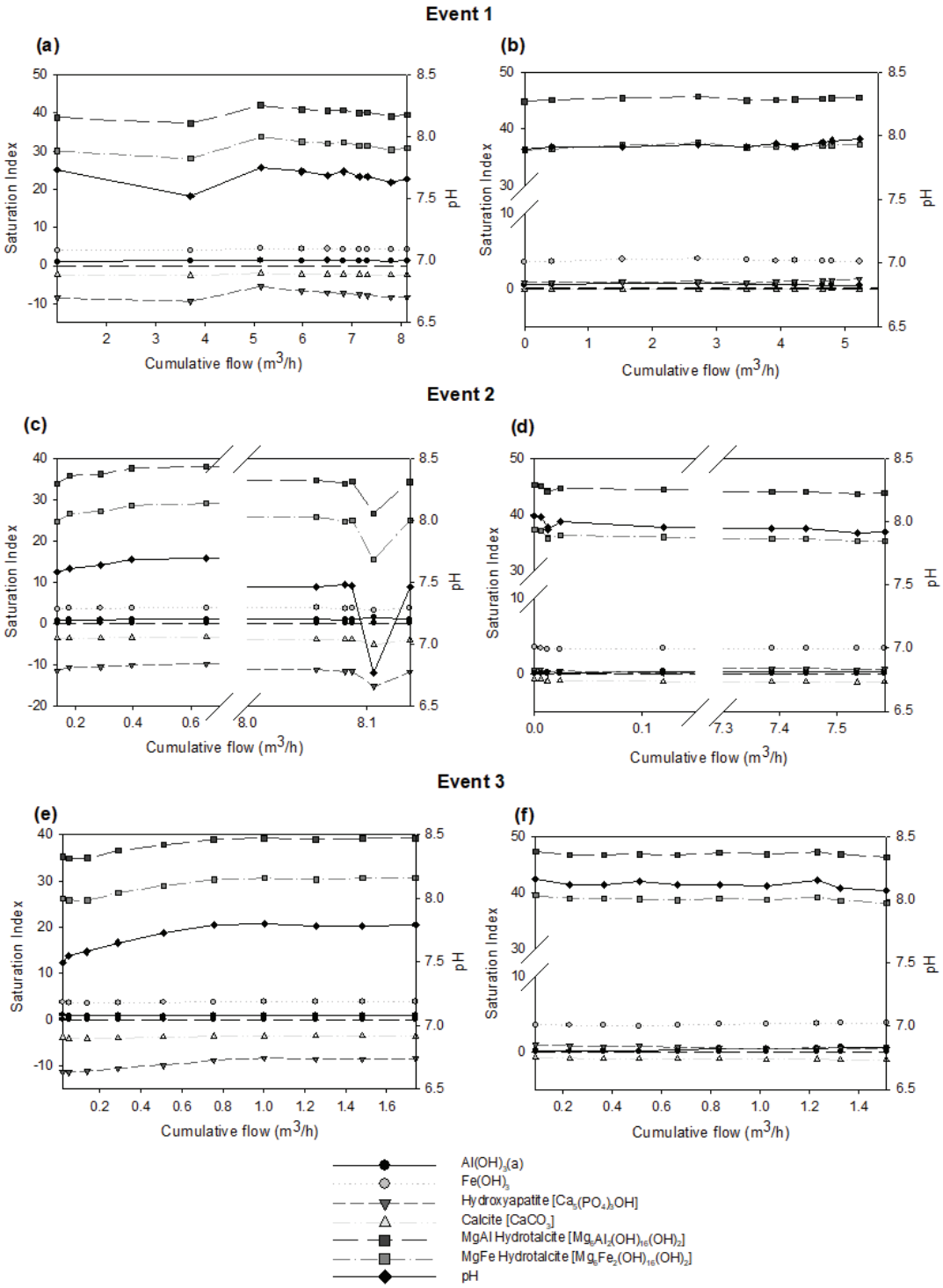

Fig. 8. Saturation indices for mineral phases likely controlling the effluent concentrations where (**a**), (**c**) and (**e**) results for sand filter, and (**b**), (**d**), (**f**) results for biochar-amended sand filter for three events respectively.

Discussion

Discharge modelling results

Hydrological processes in the filter were simulated with the STYX model including accumulation of water from precipitation in the surface domain, and unsaturated and saturated water flow in the filter subsurface domain. According to the simulation results, the discharge data were successfully recorded except for some missing events in the biochar amended filter. Simulations showed neither leakage from the structures nor prolonged waterlogged conditions inside the filters. Anoxic conditions could increase solute dissolution from the filter material, which was evident in the PHREEQC simulation results.

An important result was that the biochar amended sand filter retained water longer than the sand filter, which reflected lower hydraulic conductivity and water retention properties of the biochar material. Previously, biochar amended filtration systems have been reported to improve water retention (Mai and Huang, 2021). Higher water retention capacity favours the presence of a saturation zone which can enhance denitrification, and the number of antecedent dry days appears to have little influence on nitrate (NH_4^+) removal (Afrooz and Boehm, 2017, Rahman *et al.*, 2020). It is possible that thicker layers of biochar can start to hydraulically block the filter when hydraulic conductivity of the material is low. STYX was applied in this study to simulate the filters from the water quantity viewpoint, but the future objective is to include water quality dynamics and couple PHREEQC model to STYX via PhreeqcRM API (Parkhurst and Wissmeier, 2015). This would enable coupled simulation of water flow, geochemistry and solute transport within the filter structure.

Sources of stormwater pollution and pollutant retention mechanisms

Typical sources of pollutants in road and street runoff include atmospheric deposition, tire abrasion and wear of vehicle components such as brakes, and the application of de-icing salts (Markiewicz *et al.*, 2017, Müller *et al.*, 2020, Järlskog *et al.*, 2021) resulting in increased concentrations of nutrients (N and P) and heavy metals (e.g., Cd, Zn, nickel (Ni), Cu) (Lundy *et al.*, 2012). The total impervious area and land use in the drainage area additionally contribute to stormwater pollutant load, which strongly varies with seasonal changes (Valtanen *et al.*, 2014). Influent stormwater samples (reference stormwater) for the study were collected from a bridge drainage opening 300 m apart from the filters. The construction materials at the bridge site (mainly concrete and steel) may have influenced the stormwater quality. Although pH and EC of the biochar amended filter was consistently higher than pH of reference stormwater, pH stayed within the 6.5–8.5 limit which is the most optimal range for the aquatic microorganisms (US EPA, 2023). Elevated EC can broadly be attributed to increasing base cation concentration due to ash dissolution in the sand-biochar filter (Tan *et al.*, 2015). The filter effluents had higher pH and EC possibly due to higher orthophosphate (PO_4^{3-}), nitrate (NO_3^-) and Cl^- concentrations relative to reference stormwater (see Supplementary Information Fig. S1).

Hydrogeochemical modelling and data shows that pollutant attenuation in both filters occurs via a combination of physical (filtering) and chemical (sorption, precipitation, transformation) mechanisms as most metals and P compounds in stormwater runoff from roads exist in particle-bound form. Sand is considered chemically inert, and the primary mode of action for sand filters is physical entrapment of particulate pollutants. Although trace mineral 'impurities' in sand used in filter construction typically contribute to a small degree of chemical reactivity, a major part of the reactivity of the filter solid phase can be attributed to the biochar component of the sand-biochar filter. Although fine filter media, such as sand, has been shown to successfully retain stormwater pollutants, such filters often exhibit inferior hydraulic capacity with time and antecedent dry periods (Hatt *et al.*, 2008).

The mineral phases determined by PHREEQC modelling as most likely controlling major ion concentrations in sand-biochar effluent via precipitation/dissolution reactions included amorphous $Al(OH)_3$, poorly crystalline $Fe(OH)_3$,

hydroxyapatite ($Ca_5(PO_4)_3OH$), calcite ($CaCO_3$), MgAl hydrotalcite ($Mg_6Al_2(OH)_{16}(OH)_2$) and MgFe hydrotalcite ($Mg_6Fe_2(OH)_{16}(OH)_2$). Both the degree of Fe oxide mineral phase saturation and the quantity of labile Ca^{2+} in filter materials had a noticeable impact on P removal from stormwater by calcium phosphate mineral formation and/or adsorption to Fe oxide mineral surfaces in sand and sand-biochar filters. The primary mechanisms of P removal from influent stormwater were thus PO_4^{3-} sorption to Fe (oxy)hydroxides or precipitation of Ca phosphate mineral phases (hydroxyapatite). Similar behaviour was reported by Tian *et al.* (2016) who demonstrated that P removal likely occurred via ion exchange, precipitation or sorption, and that presence of cations (Ca^{2+} and Mg^{2+}) impacted P sorption and removal of Ca^{2+} through precipitation of hydroxyapatite. Sø *et al.* (2011) demonstrated the rapid PO_4^{3-} sorption onto calcite which can act as both the source and sink for PO_4^{3-} due to a similarly rapid dissolution rate. PHREEQC modelling showed that both calcite and hydroxyapatite were theoretically oversaturated or near-equilibrium at 5°C (Fig. 8). Although PHREEQC model results indicate oversaturation, the formation of schwertmannite is unlikely as it forms at acidic pH and significantly higher sulphate concentrations than observed herein (Zhang *et al.*, 2017).

Based on findings by Koivusalo *et al.* (2023), the sand filter showed the elevated concentrations of NO_3-N, TN and Cl^- and biochar amended sand filter demonstrated higher NH_4-N and TN removal. This is consistent with findings by Rahman *et al.* (2020) who observed saturated conditions at the bottom of a biochar column that facilitated denitrification and TN removal. Additionally, cations such as K^+, Ca^{2+} and Mg^{2+} and anions such as Cl^- present in stormwater may influence biochar adsorption of NH_4^+ and PO_4^{3-} (Zhang *et al.*, 2020). Modelling with STYX, however, demonstrated no saturated conditions (cf. Discharge modelling results section) although biochar-amended sand filter retained water for longer time than the sand filter. Detailed investigations using moisture sensors could clarify the development of saturated conditions inside the biochar-amended filter.

Leaching or dissolution of cations, particularly Ca^{2+}, Mg^{2+}, Fe^{2+} and Al^{3+}, from the sand-biochar solid phase contributed to pollutant adsorption by enabling the formation of new minerals within the filter matrix. The results further indicate the contribution of the biochar amended filter to increased TP concentrations, which can be attributed to reduced availability of binding sites on the biochar after two years of continuous operation or leaching of the fine biochar material (Hale *et al.*, 2013). Mukherjee and Zimmerman (2013) reported P losses from wood and grass biochar which were related to the ash content and acid functional groups in biochar material, indicating that weak acids can enhance the solubility of P adsorbed in Fe-, Al- and Ca-minerals and that P in biochar is bound in the ash fraction.

The results indicate oversaturation of common Fe mineral phases ferrihydrite, goethite, hematite and schwertmannite. Some studies suggest that surface-bound ferrous iron (Fe^{2+}) is significantly more reactive than dissolved ferrous iron (e.g., Larese-Casanova *et al.*, 2012). Poorly crystalline Fe oxyhydroxide, or ferrihydrite, was the mineral phase most likely controlling P attenuation via P-Fe complexation due to the relatively rapid kinetics of poorly crystalline Fe mineral formation. Concentrations of Pb and Zn within influent stormwater and the effluents of both sand and sand/biochar filters were consistent with well-defined solubility and cation exchange characteristics of these metals, and with results obtained in 2017 (Assmuth *et al.*, 2019).

The data demonstrated retention of Zn, Cu and Cd and simultaneous leaching and increased outlet concentrations of alkali metals, PO_4^{3-} and Al. The greater Zn adsorption capacity of the sand-biochar filter can be attributed to more alkaline conditions influenced by pH-dependant biochar surface charge (Tan *et al.*, 2015). The most significant difference between 2017 and 2019 results was the decrease in TP and PO_4^{3-} removal by the sand-biochar filter (see Koivusalo *et al.*, 2023) indicating declining P sorption capacity. Similar biochar behaviour was reported by Wendling *et al.* (2013) and Zhang *et al.* (2017). This behaviour is most likely due to a decrease in labile Ca^{2+} ions within the sand-biochar matrix with time.

It should be noted that the results of the present study represent one type of biochar, manufactured from birch, which is not the typical feedstock source for stormwater applications (Biswal *et al.*, 2022). The comparison to the results of other biochar feedstocks should be attributable to the properties of biochar in question. The main comparison for this study is Assmuth *et al.* (2019) who applied the Event Mean Concentration (EMC) approach for determining the pollutant removal efficiencies and mineral saturation indices of both filters. The present study used individual values for producing the saturation indices which rendered a more diverse representation of filters' dynamics. Assmuth *et al.* (2019) similarly reported near-equilibrium of hydroxyapatite and poor PO_4^{3-} removal for biochar amended filter. Of note, they observed that TP removal was consistent, which was not observed in the present study.

Previous investigation of birch biochar performance in column trials are corresponding to the biochar behaviour in the field. The same material demonstrated high retention of metals such as Zn, Cu and Pb at the same time leaching PO_4^{3-} during the column trials (Wendling *et al.*, 2017). Other investigations of birch biochar performance, to the author's knowledge, include only Kuoppamäki *et al.* (2019) who similarly observed TN leaching from birch biochar after irrigation with artificial stormwater. The primary difference to the present study was the high retention of P and the poor retention of TN by Kuoppamäki *et al.* (2019), where a significant proportion of both TP and TN were attributed to immobilisation by plant biomass. Kuoppamäki *et al.* (2019) also reported retention of Cr, Pb, and Cu, and release of Zn, which was similar in the present results.

The absence of the evaluation of the role of microbiological activity in pollutant removal additionally adds to the ambiguity as no core samples were taken from the filters to ensure the integrity of the layering. The assumption that the layering of the filter media had not significantly changed after filter construction may not be valid. Biochar has been noted for changing the soil microbial ecology and community composition to one that promotes NH_4^+ reduction (nitrification) as well as bacterial PO_4^{3-} solubilisation (Anderson *et al.*, 2011).

Long-term filters suitability for stormwater treatment

Building upon the results detailed in this study, it is possible to evaluate the conditions that are most likely to disrupt stormwater filter performance. Iron mineral phases (ferrihydrite, goethite, hematite and schwertmannite) were theoretically oversaturated in filter effluents, indicating that the *in-situ* formation of these mineral phases likely played a key role in pollutant removal. In contrast to aluminium (hydr)oxides and aluminosilicate mineral phases, Fe and Mn minerals are strongly affected by changes in oxidative-reductive potential.

For example, when Fe^{2+} is oxidised to Fe^{3+}, poorly crystalline iron (oxy)hydroxide minerals precipitate from solution, providing a reactive surface area for cationic pollutant retention. Metals may also form surface precipitates on the newly formed Fe oxide and (oxy)hydroxide mineral phases or may co-precipitate with Fe in mixed oxide phases. The opposite process occurs when Fe^{3+} is reduced to Fe^{2+} following prolonged waterlogging. The dissolution of Fe (oxy)hydroxide mineral phases under chemically reducing conditions can release previously retained cationic pollutants in a 'flush', observed as a spike in concentration of soluble Fe and metal/metalloid pollutants in filter effluent. For this reason, where (ad)sorption to Fe and/or Mn oxide and (oxy) hydroxide mineral phases is a primary mechanism of pollutant attenuation, it is critical to ensure that water does not remain standing within the filter for a prolonged period such that the rate of oxygen consumption is greater than the rate of oxygen diffusion, leading to mineral dissolution.

Clogging and the reduction of the filter hydraulic conductivity as a result of particle accumulation within the top layer of the filter depends, among other factors, on the stormwater particle size and stormwater loading rate (Kandra *et al.*, 2015). Clogging may be influenced by metal precipitates or other large solid particles. Inflow and infiltration rates impacted by the hydraulic conductivity have been shown to influence TN and TP effluent concentrations (Zhang *et al.*, 2020). The development of biofilm as the filters age over time has shown a reduction of bacterial removal but at the same time increased the removal of

nutrients (Afrooz and Boehm, 2017). Presence of vegetation has been demonstrated to reduce clogging and maintain permeability over time which is also applicable to the cold climate conditions (Le Coustumer *et al.*, 2012, Valtanen *et al.*, 2017). For a more robust functioning, the design of the biochar-amended stormwater filtration systems should consider the filter media and its feedstock origin as well as production conditions, catchment type, its area and activities within the catchment which influence the particle size distribution in stormwater, as well as the conditions that impact the ions removal such as the antecedent dry days and the presence of a saturated zone (Kandra *et al.*, 2015, Sillanpää and Koivusalo, 2015).

Conclusions

The water quality data of sand and sand-biochar filters had suggested that both filters were successful at retaining metals, such as Pb and Zn (Koivusalo *et al.* 2023). However, biochar amended filter leached K, TOC, Cl, Mg, and Ca, while showing high NH_4-N and TN removal. The sand filter effluent had elevated concentrations of NO_3-N, TN and Cl^- during high intensity rain events.

Geochemical modelling provides insights into the theoretical thermodynamic stability of potential mineral phases, thus informing the conditions that are most likely to alter the filter performance. The interactions between stormwater pollutants and the filter materials aid in evaluating the likely long-term performance of stormwater filtration systems with respect to ambient conditions. The mineral phases identified as most likely controlling major ion concentrations in biochar-amended sand filter effluents were amorphous $Al(OH)_3$, poorly crystalline $Fe(OH)_3$, hydroxyapatite ($Ca_5(PO_4)_3OH$), calcite ($CaCO_3$), MgAl hydrotalcite ($Mg_6Al_2(OH)_{16}(OH)_2$) and MgFe hydrotalcite ($Mg_6Fe_2(OH)_{16}(OH)_2$).

In the present study, (ad)sorption to Fe and/or Mn oxide and (oxy)hydroxide mineral phases was the primary mechanism of pollutant attenuation, and as such it is critical to ensure that water does not remain standing within the filter for a prolonged period. Thus, optimal maintenance of filters for long-term performance should include monitoring of oxidative-reductive potential. Such waterlogging can result in a rate of oxygen consumption that is greater than the rate of oxygen diffusion, leading to mineral dissolution.

Assessment of the microbiological activity within the filtration systems was beyond the scope of the present study. Thus, the functional diversity of microbial species within the stormwater filters remains unknown along with their contribution to stormwater purification. Analyses of 2019 sand-biochar filter effluents showed elevated P and alkali metal concentrations relative to 2017 values, whilst modelling using STYX indicated that the sand-biochar filter retained relatively greater runoff volumes than the sand filter system. Multiple parameters should be considered for a biochar-amended stormwater filtration system design including the characteristics of the catchment, biochar media as well as factors that promote filter clogging over time.

Further examination of long-term extended analyses using STYX-PHREEQC are needed to estimate stormwater filter performance, maintenance interval and lifetime under changing climate conditions. The model could also be used for optimising the filter structure by adjusting layer depths, material and drainage system properties to find the most cost-efficient and hydraulically effective configuration. This can have a notable effect in stormwater management when filters are installed in greater numbers or at larger scale along roads.

Acknowledgements: The authors would like to acknowledge the experimental field work for the measurement campaigns by Andrew Said. This research was funded by the Academy of Finland (326787), EU Water JPI – EviBAN project (Evidence based assessment of NWRM for sustainable water management).

Author contribution: Conceptualization, M.D., L.Wa. and L.We.; methodology, M.D., L.Wa. and L.We.; formal analysis, M.D.; data curation, M.D. and L.Wa.; writing — original draft preparation, M.D., L.We. and L.Wa.; writing — review and editing, M.D., L.Wa., O.T., L.We., V.R.-H., H.K.; visualization, M.D. and L.Wa.; project administration, H.K. and L.We.; funding acquisition, H.K. and L.We. All authors have read and agreed to the published version of the manuscript.

Supplementary Information: The supplementary information related to this article is available online at: http://www.borenv.net/BER/archive/pdfs/ber29/ber29-017-034-supplement.pdf

References

Afrooz, A. N., & Boehm, A. B. (2017). Effects of submerged zone, media aging, and antecedent dry period on the performance of biochar-amended biofilters in removing fecal indicators and nutrients from natural stormwater. *Ecological Engineering*, *102*, 320-330.

Ahmad, M., Rajapaksha, A. U., Lim, J. E., Zhang, M., Bolan, N., Mohan, D., ... & Ok, Y. S. (2014). Biochar as a sorbent for contaminant management in soil and water: a review. *Chemosphere*, *99*, 19-33.

Anderson, C. R., Condron, L. M., Clough, T. J., Fiers, M., Stewart, A., Hill, R. A., & Sherlock, R. R. (2011). Biochar induced soil microbial community change: implications for biogeochemical cycling of carbon, nitrogen and phosphorus. *Pedobiologia*, *54*(5-6), 309-320.

Appelo, C. A. J. & Postma, D. (2007). *Geochemistry, groundwater and pollution*. A.A. Balkema Publishers, Leiden.

Ashoori, N., Teixido, M., Spahr, S., LeFevre, G. H., Sedlak, D. L., & Luthy, R. G. (2019). Evaluation of pilot-scale biochar-amended woodchip bioreactors to remove nitrate, metals, and trace organic contaminants from urban stormwater runoff. *Water Research*, 154, 1–11.

Assmuth, E., Sillanpää, N., Wendling, L. & Koivusalo, H. (2019). Impact of Biochar on Treatment Performance of Roadside Sand Filters – Field Monitoring and Geochemical Modelling. In: *Green Energy and Technology,* G. Mannina. (ed.), Springer Verlag, pp. 79–84.

Bäckström, M., Nilsson, U., Håkansson, K., Allard, B. & Karlsson, S. (2003). Speciation of heavy metals in road runoff and roadside total deposition. *Water, Air, and Soil Pollution*, 147, 343–366.

Biswal, B. K., Vijayaraghavan, K., Tsen-Tieng, D. L., & Balasubramanian, R. (2022). Biochar-based bioretention systems for removal of chemical and microbial pollutants from stormwater: A critical review. *Journal of Hazardous Materials*, *422*, 126886.

Boehm, A. B., Bell, C. D., Fitzgerald, N. J., Gallo, E., Higgins, C. P., Hogue, T. S., ... & Wolfand, J. M. (2020). Biochar-augmented biofilters to improve pollutant removal from stormwater–can they improve receiving water quality?. *Environmental Science: Water Research & Technology*, *6*(6), 1520-1537.

Doherty, J. (2010). *PEST – Model-independent Parameter Estimation User Manual*, 5th ed. Watermark Numerical Computing.

Fletcher, T. D., Shuster, W., Hunt, W. F., Ashley, R., Butler, D., Arthur, S., Trowsdale, S., Barraud, S., Semadeni-Davies, A., Bertrand-Krajewski, J.-L., Mikkelsen, P. S., Rivard, G., Uhl, M., Dagenais, D., & Viklander, M. (2015). SUDS, LID, BMPs, WSUD and more – The evolution and application of terminology surrounding urban drainage. *Urban Water Journal*, 12(7), 525–542.

Genç-Fuhrman, H., Mikkelsen, P. S., & Ledin, A. (2007). Simultaneous removal of As, Cd, Cr, Cu, Ni and Zn from stormwater: Experimental comparison of 11 different sorbents. *Water Research*, 41(3), 591–602.

Hale, S. E., Alling, V., Martinsen, V., Mulder, J., Breedveld, G. D., & Cornelissen, G. (2013). The sorption and desorption of phosphate-P, ammonium-N and nitrate-N in cacao shell and corn cob biochars. *Chemosphere*, *91*(11), 1612-1619.

Hargreaves, G. H. & Allen, R. G. (2003). History and Evaluation of Hargreaves Evapotranspiration Equation. *Journal of Irrigation and Drainage Engineering*, 129, 53-63.

Hatt, B. E., Fletcher, T. D., & Deletic, A. (2008). Hydraulic and Pollutant Removal Performance of Fine Media Stormwater Filtration Systems. *Environmental Science & Technology*, 42(7), 2535–2541.

Järlskog, I., Strömvall, A.-M., Magnusson, K., Galfi, H., Björklund, K., Polukarova, M., Garção, R., Markiewicz, A., Aronsson, M., Gustafsson, M., Norin, M., Blom, L. & Andersson-Sköld, Y. (2021). Traffic-related microplastic particles, metals, and organic pollutants in an urban area under reconstruction. *Science of The Total Environment*, 774, 145503.

Kandra, H., McCarthy, D., & Deletic, A. (2015). Assessment of the impact of stormwater characteristics on clogging in stormwater filters. *Water resources management*, *29*, 1031-1048.

Kaya, D., Croft, K., Pamuru, S. T., Yuan, C., Davis, A. P., & Kjellerup, B. V. (2022). Considerations for evaluating innovative stormwater treatment media for removal of dissolved contaminants of concern with focus on biochar. *Chemosphere*, *307*, 135753.

Koivusalo, H., Dubovik, M., Wendling, L., Assmuth, E., Sillanpää, N., & Kokkonen, T. (2023). Performance of sand and mixed sand-biochar filters for treatment of road runoff quantity and quality. *Water*, 15(8), 1631.

Kołodyńska, D., Wnętrzak, R., Leahy, J. J., Hayes, M. H. B., Kwapiński, W., & Hubicki, Z. J. C. E. J. (2012). Kinetic and adsorptive characterization of biochar in metal ions removal. *Chemical Engineering Journal*, *197*, 295-305.

Komkiene, J., & Baltrenaite, E. (2016). Biochar as adsorbent for removal of heavy metal ions [Cadmium (II), Copper (II), Lead (II), Zinc (II)] from aqueous phase. *International Journal of Environmental Science and Technology*, *13*, 471-482.

Kuoppamäki, K., & Lehvävirta, S. (2016). Mitigating nutrient leaching from green roofs with biochar. *Landscape and Urban Planning*, *152*, 39-48.

Kuoppamäki, K., Hagner, M., Valtanen, M. & Setälä, H. (2019). Using biochar to purify runoff in road verges of urbanised watersheds: A large-scale field lysimeter study. *Watershed Ecology and the Environment*, 1, 15–25.

Larese-Casanova, P., Kappler, A., & Haderlein, S. B. (2012). Heterogeneous oxidation of Fe(II) on iron oxides in aqueous systems: Identification and controls of Fe(III) product formation. *Geochimica et Cosmochimica Acta*, 91, 171–186.

Le Coustumer, S., Fletcher, T. D., Deletic, A., Barraud, S., & Poelsma, P. (2012). The influence of design parameters on clogging of stormwater biofilters: A large-scale column study. *Water Research*, *46*(20), 6743-6752.

Lehmann, J., & Joseph, S. (2009). Biochar for Environmental Management: An introduction. In J. Lehmann & S. Joseph (Eds.), *Biochar for Environmental Management* (2nd ed., p. 976). Routledge.

Liao, W., Drake, J., & Thomas, S. C. (2022). Biochar granulation, particle size, and vegetation effects on leachate water quality from a green roof substrate. *Journal of Environmental Management*, *318*, 115506.

Lundy, L., Ellis, J. B., & Revitt, D. M. (2012). Risk prioritisation of stormwater pollutant sources. *Water Research*, 46(20), 6589–6600.

Mai, Y., & Huang, G. (2021). Hydrology and rainfall runoff pollutant removal performance of biochar-amended bioretention facilities based on field-scale experiments in lateritic red soil regions. *Science of The Total Environment*, *761*, 143252.

Markiewicz, A., Björklund, K., Eriksson, E., Kalmykova, Y., Strömvall, A.-M., & Siopi, A. (2017). Emissions of organic pollutants from traffic and roads: Priority pollutants selection and substance flow analysis. *Science of The Total Environment*, 580, 1162–1174.

Mohanty, S. K., Cantrell, K. B., Nelson, K. L., & Boehm, A. B. (2014). Efficacy of biochar to remove Escherichia coli from stormwater under steady and intermittent flow. *Water Research*, *61*, 288–296.

Mohanty, S. K., Valenca, R., Berger, A. W., Yu, I. K. M., Xiong, X., Saunders, T. M., & Tsang, D. C. W. (2018). Plenty of room for carbon on the ground: Potential applications of biochar for stormwater treatment. *Science of The Total Environment*, 625, 1644–1658.

Mukherjee, A., & Zimmerman, A. R. (2013). Organic carbon and nutrient release from a range of laboratory-produced biochars and biochar–soil mixtures. *Geoderma*, *193*, 122-130.

Müller, A., Österlund, H., Marsalek, J., & Viklander, M. (2020). The pollution conveyed by urban runoff: A review of sources. *Science of The Total Environment*, *709*, 136125.

Nash, J.E. & Sutcliffe, J.V. (1970). River flow forecasting through conceptual models part I — A discussion of principles. *Journal of Hydrology*, 10(3), 282–290.

Owens, P. N., & Walling, D. E. (2002). The phosphorus content of fluvial sediment in rural and industrialized river basins. *Water Research*, 36(3), 685–701.

Parkhurst, D.L., & Wissmeier, L., (2015). *PhreeqcRM: A reaction module for transport simulators based on the geochemical model PHREEQC*.

Rahman, M.Y.A., Nachabe, M.H., & Ergas, S.J. (2020). Biochar amendment of stormwater bioretention systems for nitrogen and Escherichia coli removal: Effect of hydraulic loading rates and antecedent dry periods. *Bioresource technology*, *310*, 123428.

Reddy, K. R., Xie, T. & Dastgheibi, S. (2014). Evaluation of Biochar as a Potential Filter Media for the Removal of Mixed Contaminants from Urban Storm Water Runoff. *Journal of Environmental Engineering*, 140(12).

Richards, L.A. (1931). Capillary conduction of liquids through porous mediums, *Physics*, 1, 318–333.

Siipola, V., Pflugmacher, S., Romar, H., Wendling, L. & Koukkari, P. (2020). Low-Cost Biochar Adsorbents for Water Purification Including Microplastics Removal. *Applied Sciences*, 10(3), 788.

Sillanpää, N., & Koivusalo, H. (2015). Stormwater quality during residential construction activities: influential variables. *Hydrological Processes*, *29*(19), 4238-4251.

Sø, H. U., Postma, D., Jakobsen, R., & Larsen, F. (2011). Sorption of phosphate onto calcite; results from batch experiments and surface complexation modeling. *Geochimica et Cosmochimica Acta*, *75*(10), 2911-2923.

Spahr, S., Teixidó, M., Gall, S. S., Pritchard, J. C., Hagemann, N., Helmreich, B., & Luthy, R. G. (2022). Performance of biochars for the elimination of trace organic contaminants and metals from urban stormwater. *Environmental Science: Water Research & Technology*, *8*(6), 1287-1299.

Taka, M., Kokkonen, T., Kuoppamäki, K., Niemi, T., Sillanpää, N., Valtanen, M., Warsta, L. & Setälä, H. (2017). Spatio-temporal patterns of major ions in urban stormwater under cold climate. *Hydrological Processes*, 31(8), 1564-1577.

Tan, X., Liu, Y., Zeng, G., Wang, X., Hu, X., Gu, Y., & Yang, Z. (2015). Application of biochar for the removal of pollutants from aqueous solutions. *Chemosphere*, 125, 70-85.

Tian, J., Miller, V., Chiu, P. C., Maresca, J. A., Guo, M., & Imhoff, P. T. (2016). Nutrient release and ammonium sorption by poultry litter and wood biochars in stormwater treatment. *Science of the Total Environment*, *553*, 596-606.

Ulrich, B. A., Loehnert, M., & Higgins, C. P. (2017). Improved contaminant removal in vegetated stormwater biofilters amended with biochar. *Environmental Science: Water Research and Technology*, *3*, 726–734.

Unites States Environmental Protection Agency (US EPA). (2023). *CADDIS Volume 2: pH*. Available at: https://www.epa.gov/caddis-vol2/ph [Accessed 12.4.2023].

Valtanen, M., Sillanpää, N., & Setälä, H. (2017). A large-scale lysimeter study of stormwater biofiltration under cold climatic conditions. *Ecological Engineering*, *100*, 89-98.

van Genuchten, M.T. (1980). A closed form equation for predicting the hydraulic conductivity of unsaturated soils, *Soil Sci. Soc. Am. J*., 44, 892–898.

Warsta, L., Karvonen, T., Koivusalo, H., Paasonen-Kivekäs, M., & Taskinen, A. (2013). Simulation of water balance in a clayey, subsurface drained agricultural field with three-dimensional FLUSH model. *Journal of Hydrology*, 476, 395–409.

Warsta, L., Turunen, M., Koivusalo, H., Paasonen-Kivekäs, M., Karvonen, T., & Taskinen, A. (2012). *Modelling heat transport and freezing and thawing processes in a clayey, subsurface drained agricultural field*. Proceedings of the International Drainage Workshop on Agricultural Drainage Needs and Future Priorities, Cairo, Egypt.

Wendling, L. A., Douglas, G. B., Coleman, S., & Yuan, Z. (2013). Nutrient and dissolved organic carbon removal from natural waters using industrial by-products. *Science of the total environment*, 442, 63-72.

Wendling, L., & Holt, E. (2020). Integrating Engineered and Nature-Based Solutions for Urban Stormwater Management. In D. J. O'Bannon (Ed.), *Women in Water Quality: Investigations by Prominent Female Engineers* (pp. 23–46). Springer.

Wendling, L., Loimula, K., Korkealaakso, J., Kuosa, H., Iitti, H., & Holt, E. (2017). *StormFilter material testing summary report: Performance of stormwater filtration systems*, Report VTT-R-05980-17, VTT, Espoo, Finland.

Xiong, J., Ren, S., He, Y., Wang, X. C., Bai, X., Wang, J., & Dzakpasu, M. (2019). Bioretention cell incorporating Fe-biochar and saturated zones for enhanced stormwater runoff treatment. *Chemosphere*, *237*, 124424.

Zhang, H., Voroney, R. P., & Price, G. W. (2017). Effects of temperature and activation on biochar chemical properties and their impact on ammonium, nitrate, and phosphate sorption. *Journal of Environmental Quality*, 46(4), 889-896.

Zhang, M., Song, G., Gelardi, D. L., Huang, L., Khan, E., Mašek, O., ... & Ok, Y. S. (2020). Evaluating biochar and its modifications for the removal of ammonium, nitrate, and phosphate in water. *Water Research*, *186*, 116303.